ウェブサイト公開用

（様式 10-1）
（海外特別研究員事業）
令和　6年　6月　30日

海外特別研究員最終報告書

独立行政法人日本学術振興会 理事長　殿

採用年度　令和4年度
受付番号　202260167
氏　　名　大木　理

海外特別研究員としての派遣期間を終了しましたので、下記のとおり報告いたします。
なお、下記及び別紙記載の内容については相違ありません。

記

1-1. 用務地（派遣先国名）用務地：　アイントホーフェン　　（国名：オランダ）

1-2. 研究課題名（和文）※研究課題名は申請時のものと違わないように記載すること。
液-液相分離によるキラル超分子ポリマーの配向制御と巨大電子スピンフイルターの開発

1-3. 派遣期間：令和　4年　4月　1日　～　令和　6年　3月　31日（731日間）

1-4. 受入研究機関名及び部局名
受入研究機関名：Eindhoven University of Technology
部局名：Institute for Complex Molecular Systems and Laboratory of Macromolecular and Organic Chemistry

1-5. 海外特別研究員の研究課題の遂行状況

Introduction

Regulating supramolecular organization of monomeric units into well-defined assemblies plays a crucial role in determining the functions of organic materials.[1] π-Conjugated chromophores are useful scaffolds for the synthesis of supramolecular materials associated with photonic and electronic properties.[2] For instance, supramolecular polymerization of amphiphilic monomers featuring C_3-symmetric conjugated cores decorated with amide-group and solubilizing alkyl chains typically forms one dimensional columnar nanostructure showing anisotropic exciton diffusion and charge transport.[3] Besides, supramolecular polymerization is associated with the asymmetry of constituent molecules. Chiral alkyl chains implemented in amphiphilic monomers leads to form supramolecular polymers with helical bias, offering spin-selective electronic functions (Chirality Induced Spin Selection: CISS).[4]

Currently, the preparation of supramolecular polymeric optoelectronic materials strongly relies on spin coating technique. It basically results in random mount of isolated fibers and/or coagulation of fibers, losing the inherent anisotropic functions at macroscale. One possible idea to overcome the gap between the solution state and the solid state is mediating liquid-liquid phase separation (LLPS) of supramolecular polymers, where constituent polymers form their dense droplets (or lyotropic liquid crystalline droplets) at large size.[5] If the droplets mesophase can be achieved, it might pave the way to handle macroscopic order of supramolecular polymers. However, although LLPS of polymers is ubiquitous in nature, no one reported LLPS from supramolecular polymers at the point of 2022. We thus proposed the demonstration of LLPS of supramolecular polymers as main target in this research proposal.

Progress and Results [1]

Since there was no rational clue for realizing LLPS of supramolecular polymers, we first explore self-assembly of a chiral zinc porphyrin (***S*-ZnP**), which was used for CISS application in our group, in a mixture of polar and apolar organic solvents based on my previous work (Figure 1a).[6] After screening various blend combinations of solvents, we found that ***S*-ZnP** formed micrometer scale droplets in a mixture of tetrachloroethylene (TCE) and acetonitrile (MeCN) at $f_{\mathrm{MeCN}} = 0.70$ (Figure 1b). However, circular dichroism (CD) and absorption spectra of the droplets showed almost CD silent and flattening absorbance, respectively, indicative of the formation of weakly coupled J-type aggregates or otherwise amorphous aggregates (Figure 1c).[7] The results above implied that the resulting spherical structures were not formed of the chiral supramolecular polymers but non (or less)-chiral aggregates of ***S*-ZnP**.

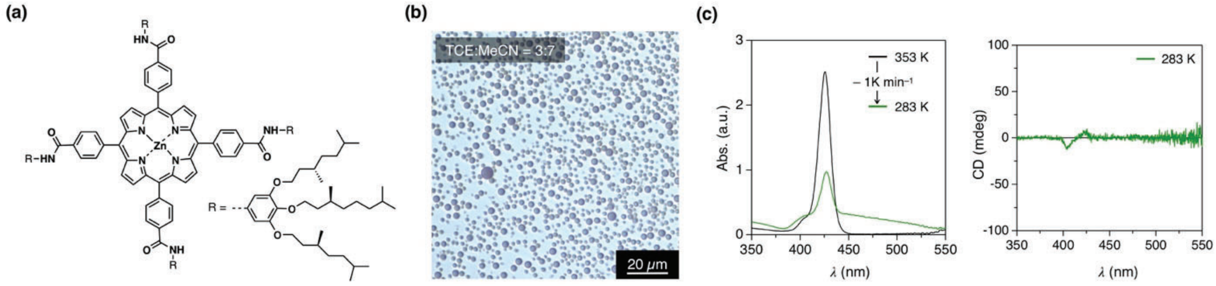

Figure 1. **(a)** Chemical structure of ***S*-ZnP** that we used as a first model monomer. **(b)** Optical micrograph of the droplets of ***S*-ZnP** formed in a mixture of TCE and MeCN ($f_{\mathrm{MeCN}} = 0.70$). **(c)** Absorption (left) and CD (right) spectra of ***S*-ZnP** in a mixture of TCE and MeCN ($f_{\mathrm{MeCN}} = 0.70$).

Afterwards, we simplified the system using single solvent because co-solvent system makes the interpretation of the role of solvents complicate. Besides, the model molecule was changed from ***S*-ZnP** to chiral triazine (***S*-T1**) and benzine (***S*-B1**) derivatives that were newly synthesized in our group (Figure 2a, top and bottom, respectively), because stronger core-core interaction can be expected than ***S*-ZnP**. First, supramolecular polymerization of ***S*-T1** and ***S*-B1** in apolar solvent was investigated by CD and UV-vis absorption spectroscopy. As a result, methylcyclohexane (MCH) solution (c = 20 μM) of **S-T1** shows a pronounced Cotton effect even at 90 °C, pointing to a significant thermal stability of the assembled polymers. The thermodynamic parameters obtained from the experimental cooling curves showed that the free energy (ΔG) values for ***S*-T1** and ***S*-B1** were –35.1 and –21.4 kJ mol^{-1}, respectively, corroborating the preferred supramolecular polymerization of ***S*-T1** than that of ***S*-B1**.

To broaden our understanding of the solute-solvent interaction along with expecting occurring of LLPS, we further investigated the supramolecular organization of ***S*-T1** and ***S*-B1** in various organic solvents. In this regard, our group recently reported a systematic approach for the rational study of the supramolecular organization of monomeric building blocks in solution based on the use of Hansen solubility parameters (HSP).[8] Following our reported methodology, 100 μM solutions of ***S*-T1** (or ***S*-B1**) in selected solvents were examined by visual inspection and CD/UV-vis absorption spectroscopy. Accordingly, the states of ***S*-T1** (***S*-B1**) were classified into four categories – namely, monomer, supramolecular polymer, meso/micro-scale assembly, and insoluble state. The obtained HSP map associated with resulting supramolecular assemblies the monomeric solvent space of ***S*-T1** is extremely narrow, while that of ***S*-B1** is compatible with typical supramolecular monomers (Figure 2b, c). These results suggested that the planarity of the conjugated core exerts a greater influence on the formation of aggregated states than dissociation by donor-acceptor interactions between solvent and solute. Intriguing is that the comparison between ***S*-T1** and an analogue of ***S*-T** featuring alkyl chain (***S*-T2**) (Figure 2a, middle). The monomer sphere of ***S*-T1** is remarkably smaller than that of ***S*-T2**. This comparison suggests that decorating the highly crystalline triazine core with trialkoxyphenyl wedges favors formation of larger-scale aggregates or even precipitation upon even a small increase in solvent polarity, because of unfavorable interactions between the aliphatic tails and polar solvents.

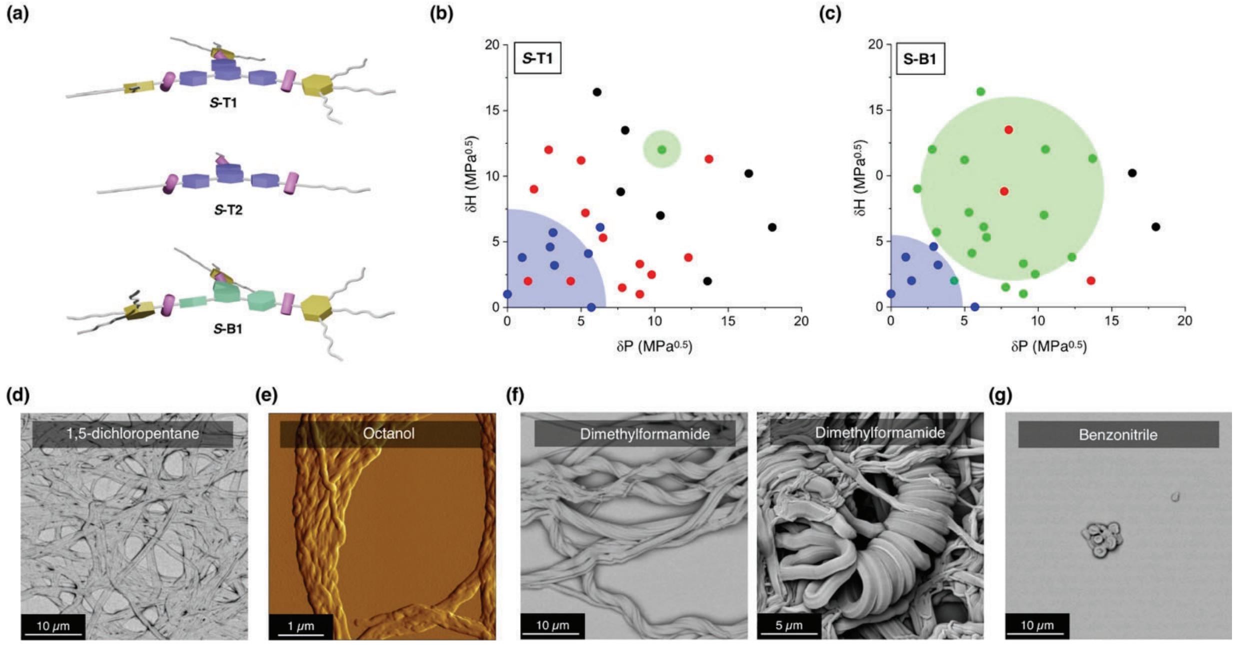

Figure 2. **(a)** Schematic representation of ***S*-T1**, ***S*-T2**, and ***S*-B1**. **(b, c)** 2D representation of Hansen solubility space for ***S*-T1** (**b**) and ***S*-B1** (**c**) at c = 100 μM observed in the $\delta_P - \delta_H$ plane. Solvents are classified as bad solvents (black dots), meso/micro-scale assembly solvents (red dots), good solvents (green dots), and SP solvents (blue dots). **(d–g)** SEM or AFM micrographs of spin coated ***S*-T1** from 1,5-dichloropentane (**d**, linear bundles), octanol (**e**, nano-helicoids), dimethylformamide (**f**, micro-helicoids/helices), and benzonitrile (**g**, globular aggregates)

To assess the influence of δ_P and δ_H on the morphology of the meso/micro-scale structures, we further characterized the supramolecular organization of ***S*-T1** under the corresponding solvent conditions. As a result of this systematic characterization, we found that the meso/micro-scale structures of ***S*-T1** can be classified into 4 categories. The most common aggregated state of ***S*-T1** is in the form of linear microstructures (Figure 2d). For instance, ***S*-T1** in 1,5-dichloropentane ($\delta_P = 7.8$, $\delta_H = 1.5$) forms elongated architectures whose spectra are characterized by single negative Cotton effect and relatively high positive LD. These observations suggest that the one-dimensional columnar structures of ***S*-T1** are bundled into straight higher-order structures, resulting in a high LD contribution. Similar linear microstructures are observed in a wide region of the δ_P-δ_H space, indicating a strong directional aggregation force of ***S*-T1**. In other words, ***S*-T1** has a strong tendency to form linearly ordered microstructures as higher-order aggregates. In contrast, ***S*-T1** in octanol ($\delta_P = 5$, $\delta_H = 11.2$) exhibits a distinct bisignate CD signal, whose intensity is four times higher than in MCH. AFM images of spin-coated samples of ***S*-T1** from octanol solutions revealed the formation of helical nano-bundles with individual widths of about 100 nm (Figure 2e). The wavy structures may rationalize the weak LD with respect to the strong CD contributions. Similarly, ***S*-T1** in dimethylformamide ($\delta_P = 13.7$, $\delta_H = 11.3$) shows an enhanced CD signal with a weak LD, but the shape of the CD differs from that of MCH and octanol solutions. SEM images show that ***S*-T1** in DMF forms left-handed helicoids and cylindrical helices in the micrometer scale (Figure 2f), indicating that the obtained CD spectrum could be strongly affected by circular differential scattering. This can be inferred from the fact that the CD intensity is present in the non-absorption region. Lastly, ***S*-T1** in benzonitrile ($\delta_P = 9.0$, $\delta_H = 3.3$) formed globular- and disc-shaped microstructures with silent CD and LD spectra (Figure 2g). These non-linear morphologies suggest that the apolar trialkoxyphenyl wedges dislike the highly polar environment and tend to minimize the aggregate surface area, resulting in the closed microstructures.

Unfortunately, we could not observe LLPS behavior for both ***S*-T1** and ***S*-B1** in any organic solvents that we used in this comprehensive study. However, our research gives the deep insight into a strong influence of the planarity of the aromatic core and the number of aliphatic chains on the supramolecular organization. We are now preparing the manuscript to discuss the impact of core and side chains design on the assembly of amide-decorated amphiphilic building blocks in the solid state and in solution. It must be noted that first demonstration of LLPS from water-soluble supramolecular polymers was reported in 2024 from our group.[9] According to the discovery, slight repulsive forces between supramolecular polymers are important to allow the fibers to be condensed but not completely bundled. Our system using aliphatic chains lacks the repulsive forces and rather promotes agglomeration of supramolecular polymers. The rational approach to realize LLPS of supramolecular polymers featuring apolar side chains is still veiled.

Progress and Results [2]

In the original proposal, we also proposed to synthesize one monomer decollating azobenzene in the side chain to light-manipulation of the supramolecular polymers. Nevertheless, we did not perform the synthesis because photoisomerization plausibly dissociate the polymer organization. Instead of the initial idea, we started to investigate a spatiotemporal control of mesophasic molecular order with using light in a platform of microdroplets made of azobenzene mesogen **RM-AzoSi$_3$** featured with Smectic liquid crystal phase at room temperature (Figure 3a).[10]

We established μ-contact printing method for preparing an array of photo-responsible microdroplets made of **RM-AzoSi$_3$**. The droplets printed on a PDMS layered surface shows a uniform POM texture featured with the four-fold symmetric Maltese cross pattern (Figure 3b). To get insight into the detail of the molecular orientation inside the droplet, a single droplet was excited with focused laser at the lowest power (λ_{ex} = 455 nm, 1mW/cm^2) and the photoluminescence was collected by a polarization camera (POLCAM) (Figure 3c). The resultant POLCAM image revealed that **RM-AzoSi$_3$** organizes the hyperbolic hedgehog structure around the central point defect inside the droplet (Figure 3d).

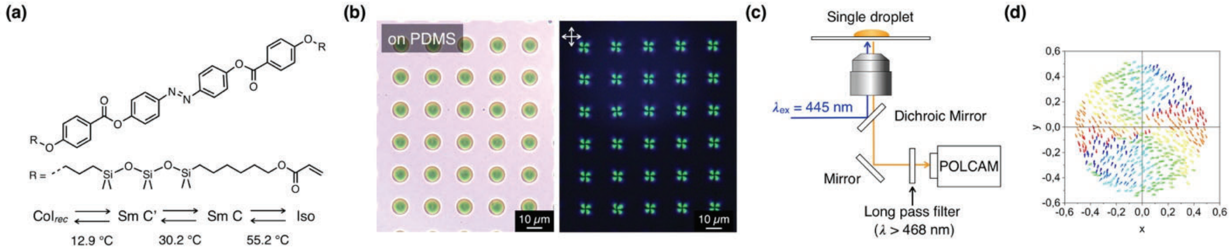

Figure 3. **(a)** Chemical structure of **RM-AzoSi$_3$**. **(b)** Optical (left) and POM (right) micrographs of the droplet array made of -**RM-AzoSi$_3$** printed on PDMS layered surface. **(c)** Schematic representation of POLCAM imaging. **(d)** Vector plots of molecular orientation inside a single droplet based on fluorescence collected by POLCAM.

To demonstrate light-manipulation of the mesophasic molecular order, a single droplet was excited with the focused polarized laser at 50 mW/cm^2 in ambient environment, and the time-course photo-orientation behavior was collected by POLCAM under weak excitation at 1.0 mW/cm^2. As a result, the intrinsic four-fold symmetric POM texture changes with respect to the laser exposure time (Figure 4a). The corresponding POLCAM images revealed that the mesophasic molecular order is directed normal to the polarization of light. The plots of anisotropy of the order showed that the light-orientation reaches plateau in 10 min (Figure 4b). Analogously, the microdroplets irradiated with different angle of polarized laser beam showed that the polarization-dependent mesophasic structure, showing the robust photo-imprinting behavior (Figure 4c). Intriguingly, although the irradiated droplet was not polymerized, the light-directed orientation was kept intact over the time. This is plausibly because the resultant mesophasic order is stabilized by the interaction at **RM-AzoSi$_3$**/PDMS interface as well as the confinement of the order in the dome geometry. Furthermore, overwriting (reversible tuning of the order) was successfully demonstrated at the identical droplet with sequential irradiation of polarized light with different angle. We are now preparing the manuscript to report the spatiotemporal control of mesophasic order in light-responsive droplets as multi-states materials.

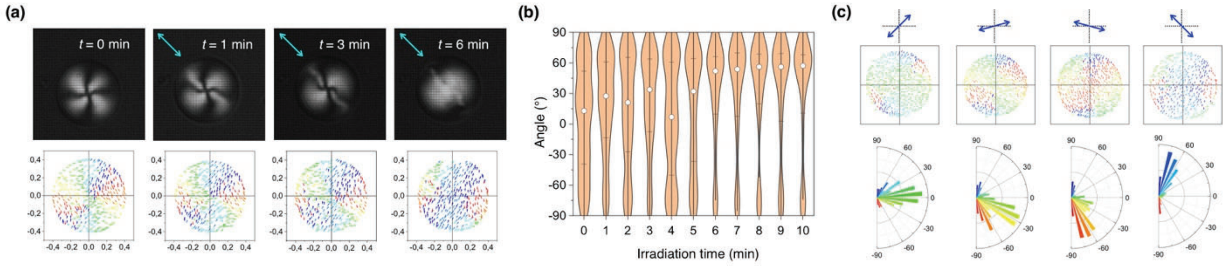

Figure 4. **(a)** POM (top) and the corresponding vector plots of the mesophasic order obtained from POLCAM imaging at different laser irradiation time. The blue arrows inside POM micrographs indicate the angle of polarization of light. **(b)** Anisotropy of the mesophasic molecular order with respect to the light irradiation time. **(c)** Vector plots obtained from the polarization angle dependent POLCAM images (top) and the corresponding radar plots of the numbers of data points with respect to the angle (bottom).

Outlook

We tried to broad our understanding of the solute-solvent interaction of supramolecular polymers along with expecting occurring of LLPS. Unfortunately, we could not achieve LLPS behavior of supramolecular polymers in organic solvents that we used. However, our microscopic and spectroscopic characterization of supramolecular assemblies revealed the strong impact of the planarity of the aromatic core and the number of aliphatic chains on the supramolecular organization both in solid and solution states. The results indicated that using aliphatic chains rather promotes agglomeration of supramolecular polymers, resulting in higher-ordered solid aggregates depending on solvent polarity. These results should shed the light on understanding of pathway complexity in supramolecular polymerization associated with their out-coming functions. Basically, all the experiments were done. We are now preparing the manuscript to report the impact of core and side chains design on the assembly. These supramolecular polymers will be tested to CISS properties in near future. In addition, we further designed the project to explore multi-states stimuli responsive materials in a platform of microdroplets made of azobenzene. We fabricated an array of the liquid crystalline microdroplets and succeeded in spatiotemporal controlling and quantifying of mesophasic order of the droplets by means of laser-integrated microscopy and POLCAM imaging, respectively. The direction of the mesophasic order is reversibly tunable upon irradiating different polarization of light. This study gives the insight into how photo-orientation occurs in mesophasic droplets visually. We are preparing the manuscript to report the spatiotemporal control of mesophasic order at a single microdroplet level.

–References–

[1] T. Aida, E. W. Meijer, S. I. Stupp, *Science* **2012**, *335*, 813–817.

[2] F. J. M. Hoeben, P. Jonkheijm, E. W. Meijer, A. P. H. J. Schenning, *Chem. Rev.* **2005**, *105*, 1491–1546.

[3] A. T. Haedler, K. Kreger, A. Issac, B. Wittmann, M. Kivala, N. Hammer, J. Köhler, H. W. Schmidt, R. Hildner, *Nature* **2015**, **523**, 196−199.

[4] C. Kulkarni, A. K. Mondal, T. K. Das, G. Grinbom, F. Tassinari, M. F. J. Mabesoone, E. W. Meijer, R. Naaman, *Adv. Mater.* **2020**, *32* (7), 1904965.

[5] P. Van de Witte, P. J. Dijksra, J. W. A. van den Berg, J. Feijen, *J. Membr. Sci.* **1996**, *117*, 1−31.

[6] W. Mtangi, F. Tassinari, K. Vankayala, A. V. Jentzsch, B. Adelizzi, A. R. A. Palmans, C. Fontanesi E. W. Meijer, R. Naaman, *J. Am. Chem. Soc.* **2017**, *139*, 7, 2794–2798.

[7] R. van der Weegen, A. J. P. Teunissen, E. W. Meijer, *Chem. -Eur. J.* **2017**, *23*, 3773–3783.

[8] J. J. B. van der Tol, G. Vantomme, E. W. Meijer, *J. Am. Chem. Soc.* **2023**, *145*, 32, 17987–17994.

[9] H. Fu, J. Huang, J.J.B.van der Tol, L. Su, Y. Wang, S. Dey, P. Zijlstra, G. Fytas, G. Vantomme, P. Y. W. Dankers, E. W. Meijer, *Nature* **2024**, *626*, 1011–1018.

[10] H. Sakaino, D. J. Broer, S. C. J. Meskers, E. W. Meijer, G. Vantomme, *Angew. Chem. Int. Ed.* **2022**, *61*, e202200839.

Acknowledgements

I would like to express my sincere appreciations to my host researcher Prof. Dr. E. W. Meijer for his great supports and encouragements to my research works. All the experience in TU/e is valuable to my life. I would like to thank Dr. Ghislaine Vantomme, for her informative suggestions and great supports to our research works. I sincerely appreciate the kind support of all the Ph.D. students, postdocs, and stuffs who has been involved in my research life in TU/e. Lastly, I'm grateful the Japan Society for the Promotion of Science for overseas research fellowships for giving me great opportunities to research in abroad.